Stark-effect study of excited states in sodium using two-photon spectroscopy*

R. T. Hawkins, W. T. Hill, F. V. Kowalski, A. L. Schawlow, and S. Svanberg†
Department of Physics, Stanford University, Stanford, California 94305
(Received 8 November 1976)

We have used two-photon absorption from counterpropagating laser beams of different frequencies to measure Stark shifts and splittings of the 6^2S, 7^2S, 8^2S, 5^2D, and 6^2D states in sodium. Beams from a fixed-frequency, single-mode Ar^+ laser and a tunable, single-frequency cw dye laser were focussed into a coarse sodium atomic beam and the fluorescence was monitored. The collimation of the atomic beam reduced the residual Doppler width inherent in using two different frequencies. Using the two lasers allowed two-photon transitions to be observed at frequencies unattainable with the dye laser alone, and enhanced the transition rates due to the near resonance of the dye laser with the strong Na $3^2S \rightarrow 3^2P$ transition. Our experimental results for the scalar and tensor polarizabilities, α_0 and α_2, agree with calculations in the Bates and Damgaard Coulomb approximation within 2% for α_0 and 9% for α_2. As a by-product the hyperfine-interaction constants a for the S states and the fine-structure intervals $\delta\nu = (E_{3/2} - E_{5/2})/h$ for the D states were obtained.

I. INTRODUCTION

During recent years, the Doppler-free two-photon spectroscopy method, which was first proposed by Vasilenko *et al.*[1] and later treated in more detail by Cagnac *et al.*,[2] has been widely used to obtain spectroscopic information on atoms and molecules. In contrast to level-crossing, antilevel-crossing, and optical double-resonance spectroscopy, two-photon spectroscopy makes possible the direct measurement of the energy of a single state, thereby allowing the study of isotope shifts and scalar Stark effects. Such Stark-effect measurements on sodium were performed some time ago in this laboratory.[3]

Recently, Bjorkholm and Liao have shown that strong resonant enhancement can be obtained in two-photon absorption by using two laser beams of different frequencies, tuned near the allowed dipole transitions involving a real intermediate state.[4] In the present paper, we report Stark-effect studies in several excited states of sodium using this near-resonant enhancement technique. A fixed-frequency, single-mode Ar^+ laser was used in conjunction with a single-mode, electronically tunable rhodamine 6G dye laser. The available tuning range was extended by using the two lasers. Moreover, the two laser wavelengths could always be reasonably close to allowed transitions to provide some enhancement of the two-photon absorption.

Operation with two lasers with considerably different frequencies results in a substantial residual Doppler width. If the frequencies of the two oppositely-directed lasers are ν_1 and ν_2, the Doppler width of the two-photon resonance is reduced by a factor $(\nu_1 - \nu_2)/(\nu_1 + \nu_2)$. Even if the laser frequencies differ by 20%, the linewidth of the resonance is reduced to 10% of the Doppler width. In the present experiment, the sodium atoms are in a crudely collimated atomic beam, which gives a further linewidth reduction. Of course, the use of an atomic beam is also very convenient in studies of the Stark interaction, since cell experiments with internal or external electric field plates are not problem-free.

The Stark effect in free atoms is due to a mixing by the electric field of states connected by electric dipole transitions. It constitutes a sensitive test of the electronic wave functions of an atom. Alkali atoms are particularly suitable for comparison with theory, because of their relatively simple electron configurations. Alkali ^2P states have been studied for some time, since dipole transitions from the ground state are possible.[5] With the introduction of new techniques, Stark studies of even-parity states have become possible. For example, two-step excitation has been used, either directly[6] or combined with level-crossing[7] or quantum beat spectroscopy.[8] As pointed out earlier, two-photon spectroscopy is also a very convenient technique for investigations of the Stark interaction.[3] Recently, Stark effect studies have also been carried out in regions where the Stark shifts are comparable to the splitting between the l states with the same principal quantum number.[9] Several studies of the Stark-field ionization process have also been performed for alkali atoms.[10]

In this paper we present experimental results for the polarizabilities of the 6^2S, 7^2S, 8^2S, 5^2D and 6^2D states, and compare them with our theoretical values based on calculations in the Bates and Damgaard Coulomb approximation.[11] We also present values for S-state hyperfine constants and D-state fine-structure intervals obtained as by-products of our Stark interaction studies of these states.

II. THEORY

A. Two-photon absorption

The theory of the strength and line shape of two-photon absorption in an atomic vapor for the case of unequal-frequency photons has been recently treated by Bjorkholm and Liao.[12] We summarize here the results from that treatment which pertain to our case of two-photon transitions with a nearly-resonant real intermediate state.

Let the oppositely-propagating laser beams have different frequencies ν_1 and ν_2. For simplicity, assume $\nu_2 \simeq \nu_{ig} \neq \nu_{fi} \simeq \nu_1$, where ν_{ig} and ν_{fi} are the frequencies of the dipole transitions connecting the atomic ground and intermediate states and the intermediate and final states, respectively. If transit time and collision effects are neglected, and the Doppler effect is assumed to be the dominant broadening factor, one obtains a transition rate with a Voigt profile centered at $\nu_1 + \nu_2 = \nu_{ig} + \nu_{fi}$. The approximate linewidth (FWHM) is

$$\Delta\nu = (\overline{v}/c)(\nu_2 - \nu_1), \tag{2.1}$$

which is the residual Doppler width of the two-photon transition in a vapor, where $\overline{v} = [8kT(\ln 2)/m]^{1/2}$.

For near-resonant two-photon transitions, "light shifts" due to the ac Stark effect must also be considered. The energy shift of an atomic level $|n\rangle$ which is induced by an optical field $\vec{\epsilon} = \vec{\epsilon}_0 \times \cos(kx - \omega t)$ is given by perturbation theory as[13]

$$\Delta E_n = \frac{1}{4} \sum_m \{ |\langle n|\vec{p}\cdot\vec{\epsilon}|m\rangle|^2 \times [(E_n - E_m - \hbar\omega)^{-1} + (E_n - E_m + \hbar\omega)^{-1}]\} . \tag{2.2}$$

As Liao and Bjorkholm point out,[14] such energy level shifts, due to virtual transitions caused by nonresonant light, are intrinsic to nonresonant two-photon processes.

B. dc Stark effect

Following the derivation of Khadjavi, Lurio, and Happer,[15] we now treat the perturbation of an atomic level by a uniform electric field. For a nondegenerate eigenstate $|n\rangle$ of the zero-field Hamiltonian H_0, the perturbation ΔE_n due to a dc electric field $\vec{\epsilon} = \epsilon\hat{z}$ to lowest order in ϵ is

$$\Delta E_n = \sum_i \frac{\langle n|\vec{\epsilon}\cdot\vec{p}|i\rangle\langle i|\vec{\epsilon}\cdot\vec{p}|n\rangle}{E_n - E_i} = \langle n|H'|n\rangle , \tag{2.3}$$

where

$$H' = \sum_i \frac{\vec{\epsilon}\cdot\vec{p}|i\rangle\langle i|\vec{\epsilon}\cdot\vec{p}}{E_n - E_i} , \tag{2.4}$$

is the effective perturbation operator. Neglecting hyperfine structure, we may label the eigenstate $|n\rangle$ by the atomic angular momentum J, its z component m_J, and any other necessary quantum numbers γ. Finally, we write the term energy difference $E_n - E_i = E(\gamma J) - E(\gamma' J')$ in the absence of external fields, obtaining the operator

$$H' = \sum_{\gamma' J' m_J'} \frac{\vec{\epsilon}\cdot\vec{p}|\gamma' J' m_J'\rangle\langle\gamma' J' m_J'|\vec{\epsilon}\cdot\vec{p}}{E(\gamma J) - E(\gamma' J')} . \tag{2.5}$$

Expanding H' in terms of irreducible operators and choosing the proper coordinates, one finds contributions from only a single component of a zeroth and a second-rank tensor. Thus we define a scalar polarizability α_0 and a tensor polarizability α_2 by

$$\Delta E_n = -\frac{\alpha_0 \epsilon^2}{2} - \frac{\alpha_2 \epsilon^2}{2} \frac{3m_J^2 - J(J+1)}{J(2J-1)} , \tag{2.6}$$

where

$$\alpha_0 = -\frac{2}{3} \sum_{J'} \frac{|\langle J||p||J'\rangle|^2}{(2J+1)[E(J) - E(J')]} , \tag{2.7}$$

$$\alpha_2 = 2\left[\frac{10J(2J-1)}{3(2J+3)(J+1)(2J+1)}\right]^{1/2} \times \sum_{J'} \frac{|\langle J||p||J'\rangle|^2}{E(J) - E(J')} (-1)^{J+J'+1} \begin{Bmatrix} J & J' & 1 \\ 1 & 2 & J \end{Bmatrix} . \tag{2.8}$$

Here $\{\cdots\}$ denotes a $6j$ symbol.

We have performed theoretical calculations for α_0 and α_2 using the Coulomb approximation of Bates and Damgaard.[11] Only the terms through $n = 11$ were used in the calculations, neglecting states nearer ionization and continuum states. These theoretical values will be presented with the experimental values for comparison.

III. EXPERIMENTAL ARRANGEMENT

The experimental arrangement used in the two-photon absorption experiment is shown in Fig. 1. One of the two lasers was a Coherent Radiation model 52G Ar^+ laser with prism line selector and temperature controlled intracavity etalon. This laser produced a single-axial-mode output at each of the visible Ar^+ laser lines from 4545 to 5145 Å. Output power in the lines we used varied from over 250 mW at 5145 Å to less than 5 mW at 4545 Å. The linewidth was generally better than 15 MHz. For some of the measurements we stabilized the Ar^+ laser to an iodine absorption line, using the Wieman-Hänsch polarization spectroscopy method[16] to provide a signal for a feedback loop coupling to the PZT-mounted Ar^+ laser output mirror. However, as the laser power used for the stabilization loop reduced the

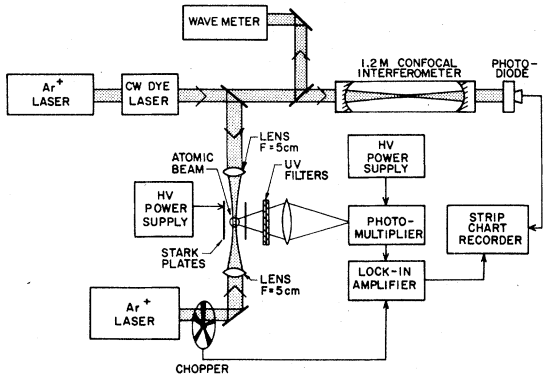

FIG. 1. Schematic of experimental apparatus.

available power for the two-photon experiment, and as the short term (< 3 min) drift was found to be negligibly small in our experiment, the stabilization arrangements were later eliminated.

The second laser was a Spectra-Physics model 580 rhodamine 6G dye-laser system which we modified for jet-stream operation. Pump power at 5145 Å was provided by a Spectra-Physics model 170 Ar^+ laser. The single-frequency dye-laser output power was typically 50 mW at 5900 Å, and the laser could be electronically tuned continuously over a maximum 4.5-GHz range. The linewidth of the laser was ~50 MHz at the outset of the experiment due to the excessive jitter caused by acoustic coupling of vibration in the water-cooling jackets of the Ar^+ lasers through the optical table to the dye laser. We managed to lower the linewidth to ~10 MHz by placing each Ar^+ laser on foam rubber cushions to acoustically decouple it from the optical table. The wavelength of the dye laser was set quickly and accurately with an interferometric digital wavemeter.[17]

The atomic-beam oven was housed in a vacuum chamber with a typical operating pressure of $\sim 10^{-5}$ Torr. The oven itself was a simple stainless steel sodium container (with a 2×5-mm slit in the top), which sat inside a boron nitride cylinder containing nichrome heater wire wound to produce minimal magnetic fields above the oven. The effusive sodium beam was collimated by another 2×5-mm slit about 2 cm above the oven exit slit. A liquid nitrogen cold trap was used for trapping the beam and improving the vacuum. The two laser beams were focussed into the atomic-beam chamber with identical 5-cm focal-length achromatic lenses, as shown in the figure. The resulting common focal point had a beam waist of about 20 μm, and was located in the center of the electric field region produced by the Stark field plates.

The field plates were basically the same ones used in an earlier Stark-effect experiment in this laboratory.[3] These Stark plates consisted of two 4×5-cm stainless steel plates separated by two 1-cm quartz spacers. The plates were thus held parallel to within ±0.005 cm, and the separation of the plates at the interaction region could be accurately determined to within ±0.0025 cm. The voltage applied across the plates was obtained from a regulated high-voltage power supply and was measured to an accuracy of 0.1%.

Two-photon absorption was detected by observing the fluorescence, in the $4\,^2P$ to $3\,^2S$ channel, through narrow parallel slits in one of the Stark plates. These slits caused negligible field inhomogeneities over the small interaction region. The RCA 8850 photomultiplier was shielded from stray light by two Corning 7-54 filters, which were not quite adequate for wavelengths below 5000 Å. Thus, some stray light from the Ar^+ laser was observed. To eliminate this background, we used lock-in detection for the weaker transitions.

The fluorescence signal was recorded, together with reference fringes from a 1.2-m confocal interferometer, on a two-pen strip chart recorder. The fringes were $c/4L$ modes of the non-mode-matched interferometer with a 64.26(2) MHz separation.

IV. EXPERIMENTAL PROCEDURE

In Fig. 2 the energy level diagram of sodium is shown. The technique used in the present two-photon absorption experiments relies upon the small wavelength difference between spectral lines connecting the $3\,^2P$ states with the studied ^2S and ^2D states and the Ar^+ laser lines in the blue-green part of the spectrum. Apart from producing strong resonant enhancement, this allows the dye laser to operate in the very favorable region

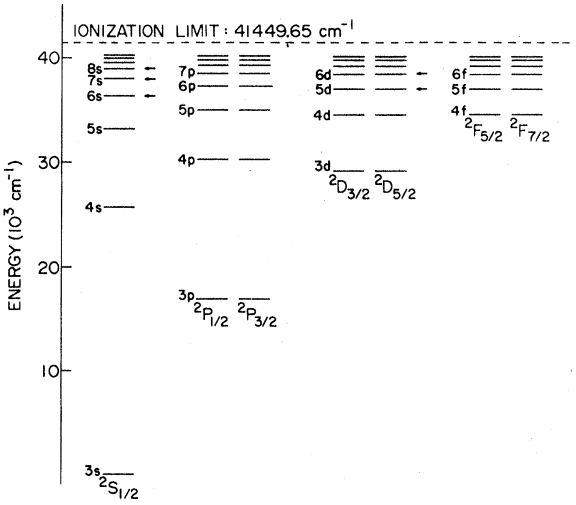

FIG. 2. Energy level diagram of atomic sodium.

TABLE I. Air wavelengths for Ar^+ and Na lines.

Na transition	λ_{Na} (Å)	λ_{Ar^+} (Å)	$\lvert\lambda_{Na}-\lambda_{Ar^+}\rvert$ (Å)	λ_{dye} (Å)
$3\,^2P_{1/2}\rightarrow 6\,^2S$	5148.8	5145.3	3.5	5900.5
$3\,^2P_{1/2}\rightarrow 5\,^2D$	4978.5	4965.1	13.5	5914.9
$3\,^2P_{3/2}\rightarrow 7\,^2S$	4751.8	4764.9	13.0	5870.0
$3\,^2P_{1/2}\rightarrow 6\,^2D$	4664.8	4657.9	6.9	5907.0
$3\,^2P_{3/2}\rightarrow 8\,^2S$	4545.22	4545.04	0.18	5890.3

$\lambda(3\,^2S_{1/2}\rightarrow 3\,^2P_{3/2}) = 5889.9$ Å; $\lambda(3\,^2S_{1/2}\rightarrow 3\,^2P_{1/2}) = 5895.9$ Å

around 5900 Å. In the figure, the arrows indicate the energies of Ar^+ laser lines, measured from the intermediate $3\,^2P$ state. In Table I, the wavelengths of the Ar^+ laser lines are compared with the corresponding resonant sodium lines for the $3\,^2P\rightarrow n\,^2S$ and $3\,^2P\rightarrow n\,^2D$ dipole transitions studied.

The signals observed in the experiments were generally quite strong due to the accidental near-resonance with a suitable Ar^+ line, and could be detected without major difficulty.

The two-photon spectrum of natural sodium is comparatively simple as there is only one stable isotope, ^{23}Na, with nuclear spin $I=\frac{3}{2}$. Further, the D states have a hyperfine structure too small to be resolvable. Thus, we were able to measure Stark-shifted ($\epsilon\neq 0$) and unshifted ($\epsilon = 0$) transitions in the same continuous scan of the dye laser frequency ν_2. The Stark shifts of all the ^2S and ^2D levels we studied were toward lower frequency, and the dye laser was only scanned toward higher frequency; so we simply turned on the electric field, scanned the dye laser through the shifted two-photon transitions, and then turned off the electric field quickly and let the scan continue through the unshifted transitions. This method was particularly favorable in that it minimized any thermally-induced drifts of either the Ar^+ laser frequency or the length of the confocal reference cavity.

It should be noted that the shifts in transition frequencies induced by the electric field are due to the combined shifts of the two states involved. However, in our case, the $3\,^2S$ ground state is shifted a completely negligible amount.[24,25] Thus, the observed shifts directly display the shifts of the upper state.

A. Measurement of ^2S states

The general structure of a sodium $^2S\rightarrow{}^2S$ transition is illustrated by the $3\,^2S_{1/2}\rightarrow 6^2S_{1/2}$ case in Fig. 3. Each $^2S_{1/2}$ state has two hyperfine levels designated by the total angular momentum quantum number $F=1$ and $F=2$. The selection rule $\Delta F = 0^2$ thus results in a pair of $3\,^2S_{1/2}\rightarrow n\,^2S_{1/2}$ two-photon transitions with the frequency difference $(\Delta\nu_{3s}-\Delta\nu_{ns})$, where $\Delta\nu_{ns}\equiv 2a_{ns}$ is the hyperfine splitting of the $n\,^2S_{1/2}$ state and $\Delta\nu_{3s}=1771.6$ MHz is the well-known ground-state hyperfine splitting.[18] In the figure, these two transition peaks are shown for the $3\,^2S_{1/2}\rightarrow 6\,^2S_{1/2}$ case. Since ^2S states exhibit only a scalar (overall) shift of all substates, as shown in Sec. II, the two peaks shift equally and remain unsplit when the electric field is applied. By switching the electric field on and off, we recorded all four peaks in the same trace.

In the figure, the observed lineshape is also further detailed. Each peak is the sum of two line profiles with different Doppler widths. The broader signal is that expected in a cell experiment, since it has the residual Doppler width (FWHM) of ~200 MHz predicted by Eq. (2.1) for the corresponding cell experiment. Actually, we observed this linewidth for this transition in preliminary cell experiments. The explanation of this broad peak in our beam experiments is simply that our vacuum and cold-trapping arrangements were not sufficient to eliminate a sodium vapor phase in the atomic-beam chamber. The narrow peak is the Doppler-narrowed contribution of the collimated atomic beam proper, and had a linewidth of about 40 MHz or less in all our observations. The small, sharp peak between the $\epsilon = 0$ and $\epsilon\neq 0$ peaks is an artifact of shutting off the voltage during the scan.

Several curves similar to the one shown in Fig.

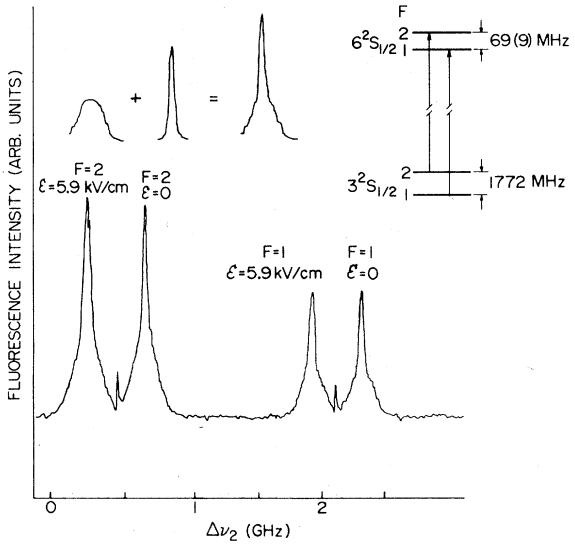

FIG. 3. Typical data curve showing Stark shifts of $6\,^2S_{1/2}$ hyperfine levels. Lineshape and expanded energy level diagram are also shown. Nonlinearity of $\Delta\nu_2$ scale is due to nonlinearity of dye laser scan.

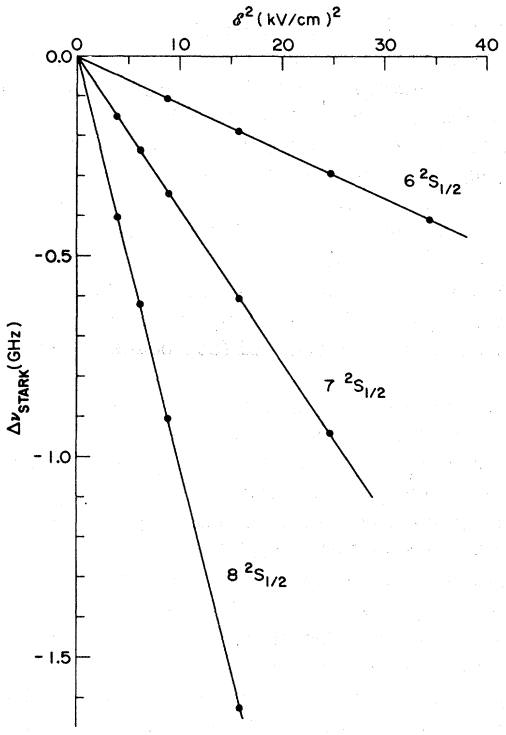

FIG. 4. Stark shifts of ^2S states measured in this experiment.

3 were taken for the 6, 7, and 8 ^2S states, varying the electric field strengths. Before and after each of the various runs, the plate separation was carefully measured. The good homogeneity of the electric field was evident from the very small broadening of even strongly-shifted signal components. For all of the transitions observed, we varied the laser powers to make sure that light shifts did not affect our results.

The results of our Stark-effect measurements for the ^2S states are shown in Fig. 4. The Stark shifts of the ^2S states are clearly quadratic in the electric field ϵ. The scalar polarizabilities and the dipole interaction constants a we measured for these states are shown in Table II. The a values were obtained by measuring the frequency separation of the two $\Delta F = 0$ two-photon transitions for each ^2S state. Given in the table are also literature values for the sequence of ^2S states, as well as theoretical values for α_0.

Although all of the two-photon transitions were reasonably enhanced, only the $3\,^2S_{1/2} \rightarrow 8\,^2S_{1/2}$ transition was sufficiently near resonance for us to observe, with our laser powers, the optically induced level shifts recently reported for the $3\,^2S \rightarrow 4\,^2D$ transition by Liao and Bjorkholm.[14] The virtual intermediate level of our transition was less than 0.9 cm^{-1} from the $3\,^2P_{3/2}$ level, and the

TABLE II. Scalar polarizabilities and hyperfine interaction constants for ^2S states of ^{23}Na. (Results are from this work except as noted.)

State	Polarizability [MHz/(kV^2/cm^2)] α_0 (exp)	α_0 (theor)	Hyperfine interaction constant a (exp) [MHz]
$3\,^2S_{1/2}$	0.0396(8)[a] 0.041(3)[b]	0.0400	885.8131(11)[d]
$4\,^2S_{1/2}$	...	0.7678	202(3)[e]
$5\,^2S_{1/2}$	5.2(3)[c]	5.384	77.6(2)[f] 79.5(3.0)[g] 78(5)[h] 75(5)[k]
$6\,^2S_{1/2}$	23.6(4)	23.36	39(3)[m] 34.5(4.5)
$7\,^2S_{1/2}$	76.4(1.2)	75.98	23.3(6.5)
$8\,^2S_{1/2}$	206(3)	203.4	...

[a]Reference 25.
[b]Reference 24.
[c]Reference 3.
[d]Reference 18.
[e]Reference 19.
[f]Reference 20.
[g]Reference 23.
[h]Reference 21.
[k]Reference 22.
[m]Reference 28.

resulting light shifts are shown in Fig. 5 for various powers of blue (4545 Å) and yellow (5890 Å) light. The full blue power is clearly too small to cause observable shifts, whereas the signals are shifted and broadened due to the yellow light intensity. The reason for this dependence can be seen in Eq. (2.2). The expressions for the shifts of the $3\,^2S_{1/2}$ and $8\,^2S_{1/2}$ level both have strong resonance denominators for the yellow and blue light, respectively. However, the corresponding matrix elements are appreciable only for the $3\,^2S \rightarrow 3\,^2P$ transitions, which have oscillator strengths about three orders of magnitude stronger than the corresponding $3\,^2P - 8\,^2S$ transitions. Thus, only the $3\,^2S$ state is shifted. The asymmetric broadening of the shifted peaks is due to the inhomogeneity of the optical-field intensity within the observed region due to the strong focussing of the laser beams.[14]

B. Measurements of D states

The fine structure in the sequence of D states in sodium is particularly interesting in that the D states are inverted. Experimental and theoretical studies of this sequence are discussed elsewhere in the literature[26,27] and will not be repeated here except to note that the inversion is attributed to strong polarization effects in non-s-type subshells of the electron core.

The Stark effects observed at moderate voltage can be larger than the ^2D state fine structure. This fact necessitates some care in the analysis of the data as the interpretation of the Stark effect in terms of scalar and tensor polarizabilities

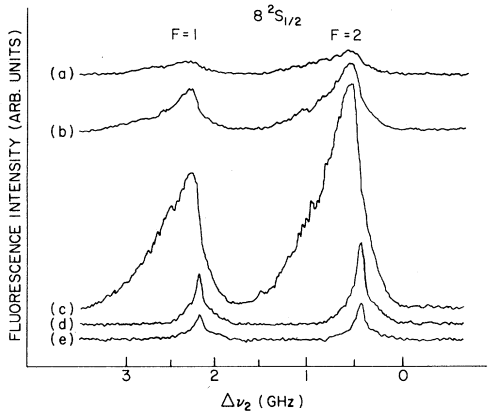

FIG. 5. ac Stark effect in $3\,^2S_{1/2} \rightarrow 8\,^2S_{1/2}$ two-photon transition. For the five traces, the powers of the blue (4545 Å) and yellow (5890 Å) lasers, respectively, were (a) 0.3-mW blue, 44-mW yellow; (b) 0.9-mW blue, 44-mW yellow; (c) 3-mW blue, 44-mW yellow; (d) 3-mW blue, 14-mW yellow; (e) 3-mW blue, 4.4-mW yellow. Relative positions of curves are only approximate.

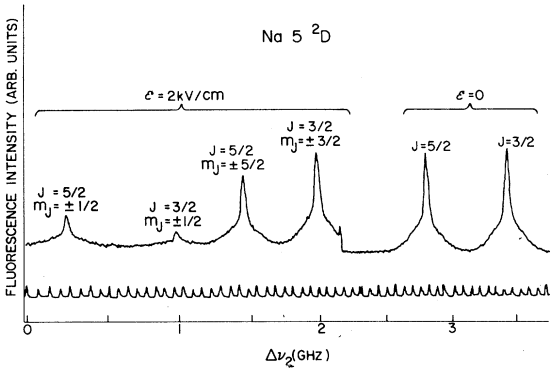

FIG. 6. Typical data curve showing Stark shifts and splittings in $3\,^2S_{1/2}$ $(F = 2) \rightarrow 5\,^2D$ two-photon transition.

assumes J to be a good quantum number, which is true only for perturbations small compared to the fine structure.

A typical data curve displaying the Stark effect in the sodium $5\,^2D$ state, as shown in Fig. 6 for the two-photon transition from the $F = 2$ hyperfine level in the ground state, reveals the general structure expected from Eq. (2.6). However, when the Stark shifts are plotted as a function of ϵ^2, as is shown in Fig. 7 for the $6\,^2D$ state, the shifts are found to be not entirely quadratic in the field. This departure from quadratic behavior is small, but present.

The lowest-order correction to Eq. (2.3) is the

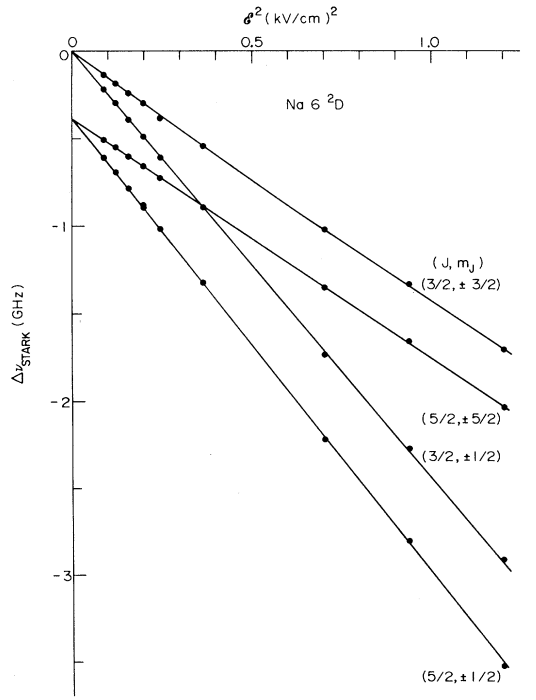

FIG. 7. Stark shifts and splittings of $6\,^2D$ state.

TABLE III. Scalar and tensor polarizabilities and fine structure intervals for ^2D states of ^{23}Na. (Results are from this work except as noted.)

State	Polarizability [MHz/(kV^2/cm^2)] α_0 (exp)	α_0 (theor)	α_2 (exp)	α_2 (theor)	Fine structure $\delta\nu$ (MHz)
$4\,^2D_{5/2}$	156.1(1.3)[a]	152.4	−53.2(5)[a]	−51.3	1028.3(6)[b] 1028.5(3.0)[c] 1025(6)[d]
$4\,^2D_{3/2}$	155.3(1.7)[a]	152.6	−38.5(7)[a]	−36.0	1035(10)[e] 1027(16)[f]
$5\,^2D_{5/2}$	1033(27)	1014	−337(21)	−330	620.0(0.6)[b] 617(10)
$5\,^2D_{3/2}$	994(23)	1015	−252(15)	−232	618(12)[g]
$6\,^2D_{5/2}$	4045(90)	3981	−1322(66)	−1290	388.02(35)[b] 385(5)[h]
$6\,^2D_{3/2}$	3985(70)	3985	−995(45)	−905	388(10)

[a]Reference 3.
[b]Reference 26.
[c]Reference 31.
[d]Reference 30.
[e]Reference 29.
[f]Reference 4.
[g]Reference 28.
[h]Reference 27.

fourth-order perturbation which is proportional to ϵ^4. We therefore empirically fit the data with a polynomial of the form

$$\Delta\nu_{\text{Stark}} = A + B\epsilon^2 + C\epsilon^4 , \tag{4.1}$$

and used the quadratic coefficient in determining the low-field polarizabilities. The values thus obtained agreed well with the values obtained by a straightforward quadratic fit to the low-field data.

The experimentally determined scalar and tensor polarizabilities, as well as the fine structure splittings $\delta\nu$ are given in Table III. The results were derived from a large number of experimental curves obtained in a way similar to that discussed for the ^2S states. Results from earlier work are given in the table for comparison where available. Further, theoretical values for α_0 and α_2, obtained with the Bates and Damgaard procedure, are included.

V. DISCUSSION

The experiments described in this paper illustrate how advantage of the powerful output of a fixed-frequency laser of suitable wavelength can be taken in two-photon absorption spectroscopy. Obtaining accurate data for the Stark interaction was clearly possible in these experiments. However, for measuring quantities like fine and hyperfine structure separations, resonance and level-crossing techniques presently give higher accuracy as their linewidth is not limited by the residual Doppler broadening and laser imperfections.

For the ^2S states, which are well isolated from adjacent states, a clear quadratic dependence on the electric field strength is observed for the Stark shifts. The accuracy of the scalar polarizabilities is within about 2%, mainly limited by electric field determination. For the ^2D states, which have a doublet structure and are quite close to adjacent states of opposite parity, the field dependence is more complicated. Our method of obtaining the strongly dominating quadratic part of the shift by a polynomial fitting procedure seems to be quite adequate. However, an additional error is introduced, and the ^2D state Stark parameters must be assigned slightly higher uncertainties.

A comparison between the experimental Stark-effect parameters and those calculated with the computer program using the Bates and Damgaard approximation shows quite good agreement. This agreement is extremely good (within 2%) for the ^2S states. The ^2D state α_0 parameters also agree well (within 2.5%), whereas the α_2 parameters deviate by as much as 9%. Despite this last deviation, the Stark effect is described well by a hydrogenic model, since it depends mainly on the wave functions in the region far from the nucleus. The fine structure, on the other hand, is sensitive to the wave function close to the nucleus and therefore displays severe deviations from the results expected in a hydrogenic model.

ACKNOWLEDGMENTS

We are grateful to John Goldsmith for his assistance in the early stages of the experiment. Also, discussions with Professor Theo.W. Hänsch and Dr. T. F. Gallagher have been very valuable in this work.

*Work supported by the National Science Foundation under Grant NSF-14789.

†Permanent address: Department of Physics, Chalmers University of Technology, S-40220 Göteborg, Sweden.

[1]L. S. Vasilenko, V. P. Chebotayev, and A. V. Shishaev, Zh. Eksp. Teor. Fiz Pisima Red. 12, 161 (1970) [JETP Lett. 12, 113 (1970)].

[2]B. Cagnac, G. Grynberg, and F. Biraben, J. Phys. (Paris) 34, 845 (1973).

[3]K. C. Harvey, R. T. Hawkins, G. Meisel, and A. L. Schawlow, Phys. Rev. Lett. 34, 1073 (1975); K. C. Harvey, Ph.D. thesis, M. L. 2442 (Stanford University, 1975) (unpublished).

[4]J. E. Bjorkholm and P. F. Liao, Phys. Rev. Lett. 33, 128 (1974).

[5]R. W. Schmieder, A. Lurio, and W. Happer, Phys. Rev. A 3, 1209 (1971).

[6]W. Fredriksson and S. Svanberg, Phys. Lett. 53A, 461 (1975); Phys. Lett. (to be published).

[7]W. Hogervorst and S. Svanberg, Phys. Lett. 48A, 89 (1974); W. Hogervorst and S. Svanberg, Phys. Scr. 12, 67 (1975); G. Belin, L. Holmgren, I. Lindgren, and S. Svanberg, Phys. Scr. 12, 287 (1975); 13, 351 (1976); 14, 39 (1976).

[8]C. Fabre and S. Haroche, Opt. Commun. 15, 254 (1975).

[9]M. G. Littman, M. I. Zimmerman, T. W. Ducas, R. R. Freeman, and D. Kleppner, Phys. Rev. Lett. 36, 788 (1976).

[10]T. W. Ducas, M. G. Littman, R. R. Freeman, and D. Kleppner, Phys. Rev. Lett. 35, 366 (1975); A. F. J. van Raan, G. Baum, and W. Raith, J. Phys. B 9, L173 (1976); L. M. Humphrey, T. F. Gallagher, S. A. Edelstein, and R. M. Hill (unpublished).

[11]D. R. Bates and A. Damgaard, Philos. Trans. R. Soc. Lond. 242, 101 (1949); the authors are grateful to W. Happer and P. Tsekeris for providing a computer program for calculating the radial integrals.

[12]J. E. Bjorkholm and P. F. Liao, Phys. Rev. A 14, 751 (1976).

[13]A. M. Bonch-Bruevich and V. A. Khodovoi, Usp. Fiz. Nauk 93, 71 (1967) [Sov. Phys.-Usp. 10, 637 (1968)].

[14]P. F. Liao and J. E. Bjorkholm, Phys. Rev. Lett. 34, 1 (1975).

[15]A. Khadjavi, A. Lurio, and W. Happer, Phys. Rev. 167, 128 (1968).

[16]C. Wieman and T. W. Hänsch, Phys. Rev. Lett. 36, 1170 (1976).

[17]F. V. Kowalski, R. T. Hawkins, and A. L. Schawlow, J. Opt. Soc. Am. 66, 965 (1976).

[18]M. Arditi and R. T. Carver, Phys. Rev. 109, 1012 (1958).

[19]K. H. Liao, R. Gupta, and W. Happer, Phys. Rev. A 8, 2811 (1973).

[20]P. Tsekeris, K. H. Liao, and R. Gupta, Phys. Rev. A 13, 2309 (1976).

[21]M. D. Levenson and N. Bloembergen, Phys. Rev. Lett. 32, 645 (1974).

[22]F. Biraben, B. Cagnac, and G. Grynberg, Phys. Lett. 49A, 71 (1974).

[23]H. T. Duong, S. Liberman, J. Pinard, and J.-L. Vialle, Phys. Rev. Lett. 33, 339 (1974).

[24]W. D. Hall and J. C. Zorn, Phys. Rev. A 10, 1141 (1974).

[25]R. W. Molof, H. L. Schwartz, T. M. Miller, and B. Bederson, Phys. Rev. A 10, 1131 (1974).

[26]K. Fredriksson and S. Svanberg, J. Phys. B 9, 1237 (1976).

[27]M. M. Salour, Opt. Commun. 18, 377 (1976).

[28]M. D. Levenson and M. M. Salour, Phys. Lett. 48A, 331 (1974).

[29]T. W. Hänsch, K. C. Harvey, G. Meisel, and A. L. Schawlow, Opt. Commun. 11, 50 (1974).

[30]D. Pritchard, J. Apt, and T. W. Ducas, Phys. Rev. Lett. 32, 641 (1974).

[31]F. Biraben, B. Cagnac, and G. Grynberg, Phys. Lett. 48A, 469 (1974).